EXPERIMENTAL FREQUENCY MAPS FOR THE ESRF STORAGE RING

Y. Papaphilippou, L. Farvacque, E. Plouviez, J.-L. Revol, A. Ropert
ESRF, Grenoble, France
J. Laskar, IMCCE, Paris France and Ch.Skokos, Academy of Athens, Greece

Abstract

Experimental frequency maps have already revealed unknown characteristics of the ESRF storage ring non-linear dynamics. In the past year, several efforts were undertaken in order to establish this technique as an operational on-line tool. The acquisition time was significantly reduced by collecting data from a dedicated fast BPM system. The problem of beam decoherence was limited by establishing a method for accurate tune determination in a small number of turns, using the information from all the BPMs around the ring. The possibility to explore the off-momentum dynamics by exciting the beam, with synchronous transverse and longitudinal kicks was also investigated.

INTRODUCTION

The frequency map analysis method [1] has been proved an efficient tool for studying theoretically [2] and experimentally [3] several aspects of non-linear beam dynamics. In particular at the ESRF storage ring, an experimental frequency map measurement campaign has started in 2002 [4], providing new insight regarding the dynamic aperture limitation of the nominal working point (0.44,0.39) and its association with a 3rd order resonance node. Other unknown beam dynamics' characteristics, as the excitation of the 5th order integer resonance close to the nominal working point, were also revealed by the method (see left part of Fig. 1). Recently, a series of improvements, with respect to beam excitation hardware, diagnostics and data analysis have been undertaken, in order to establish the frequency map analysis method as an on-line operation tool, regarding resonance analysis and correction. To this

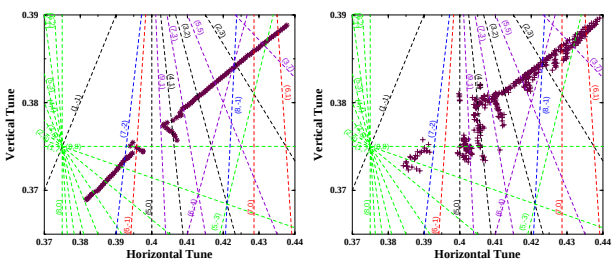

Figure 1: Frequency map for the ESRF storage ring for the nominal sextupole correction (left) and with a detuned sextupole (right).

end, the vertical shaker was refurbished and a new vertical kicker was installed with increased maximum excitation capabilities. A dedicated frequency map BPM system (ADAS) was tested successfully and reduced significantly the acquisition time, as compared to the standard 1000-turn system (MTOUR) [5]. In order to solve the problem of decoherence, a method of analysis using data from all symmetric BPMs around the ring was studied. Finally, experiments with longitudinal excitation of the beam were also performed and showed a great potential in measuring several transverse beam properties, such as off-momentum beta and dispersion variation, second order dispersion or chromaticity.

HARDWARE IMPROVEMENTS

Table 1: Kicker parameters.

Type	Hor. Kicker	Vert. Shaker	Vert. Kicker	Phase Shifter
Pulse length [μs]	1	1	1	Output of the
Rep. rate [Hz]	10	< 100	10	master source
Defl. angle [mrad]	> 2	0.1	0.6	with large
β_x,β_y [m]	5	35	35	kicks but no
Max. ampl. [mm]	10	3.5	7	calibration.

Four different equipments producing the necessary beam excitation are available in the storage ring, enabling the experimental exploration of the full 6D phase space: an horizontal injection kicker, the vertical tune-monitor shaker, a dedicated vertical kicker and an RF phase shifter. Some of their basic parameters are presented in Table 1. Note that both horizontal and vertical maximum kicker amplitudes of 10 and 7 mm are limited due to the dynamic and physical aperture, respectively, and not to the kicker hardware.

Table 2: Beam Position Monitors' parameters.

Type	Standard	"ADAS"
Number	214	1
Resolution [μm]	1 (after aver.)	2.5
Calibration	Yes	No
Linearity	Good	Limited
Acquisition speed [s/meas.]	90	1
Averaging	all BPMs	20 samples / turn

The turn-by-turn (TBT) data is recorded in two types of BPM systems: the standard MTOUR [5] and the new "ADAS" system (Table 2). The system's basic idea is to use a fast ADC board (12 bits, 64 samples per turn) to record up to 1000 turns and get one tune value per kicker pulse to radically speed up the frequency mapping scans by almost two orders of magnitude with respect to the MTOUR system. The tune monitor BPMs have the highest resolution (without averaging) but their calibration is limited. Nevertheless, this is not a major concern for tune measurements. As the amplitude detuning of the storage ring comes mostly from the horizontal excursion of the beam (Fig. 1), the tune monitor BPM block of cell 4, in particular, is very good for frequency map production, due to its high vertical and low horizontal beta. Moreover, as the frequency maps are

produced with a bunch train filling one third of the ring, there are around 20 position samples per turn which can be used for position or tune averaging. This is shown in Fig. 2, where the maximum horizontal amplitude is plotted versus all available position samples, along with the horizontal tune and betatron phase.

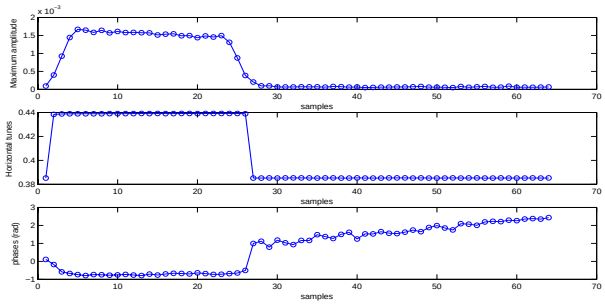

Figure 2: Maximum horizontal amplitude in mm as measured by the fast BPM system (ADAS board) (top), tune (middle) and phase (bottom) versus the sample index.

A frequency map, as the one in the right part of Fig. 1, can be produced with the ADAS system in less than 10 minutes and the acquisition speed is presently limited by kicker timing issues. These measurements were taken by applying 100 horizontal of up to 10 mm and 5 sets of vertical kicks of up to 2 mm and a detuned sextupole correction. High order two dimensional resonances appear to be excited. The frequency space is very distorted, and the dynamic aperture is limited near the area of the 5th order resonance. This provides a first example of how the frequency map can be used as a guide to understand the impact of different machine settings in the beam stability. Another application of the ADAS system is shown in Fig. 3, where off-momentum frequency maps are produced, for zero chromaticity. The momentum spread is varied from -2.5 to 2% with a step 0.5%. The horizontal tune dependence to the momentum spread is almost symmetric and the vertical tune is practically unchanged (bottom left). This symmetry is also reflected in the maximum possible horizontal kick amplitude (top left), where the minimum corresponds to ± 2 %. The frequency map shows that for $\delta p/p = 0.5$ and 1% (deep blue and green curves), the 5th order resonance is less distorted than in the case of the corresponding negative momentum spreads (light blue and green). For $\delta p/p = \pm 1.5\%$ (pink), the distortion appears due to the coupling resonance. The dip of the dynamic aperture corresponds to the crossing of 8th order resonances. Finally, the proximity to the (3,0) resonance limits the off-momentum dynamic aperture at $\delta p/p = -2.5\%$.

TUNE FROM SYMMETRIC BPM DATA

A common problem in TBT data analysis is decoherence: once the beam is kicked to high amplitude, it decoheres rapidly due to finite tune-spread, leaving a limited number of turns with signal above the noise level. A similar problem occurs with non-zero chromaticity, which adds

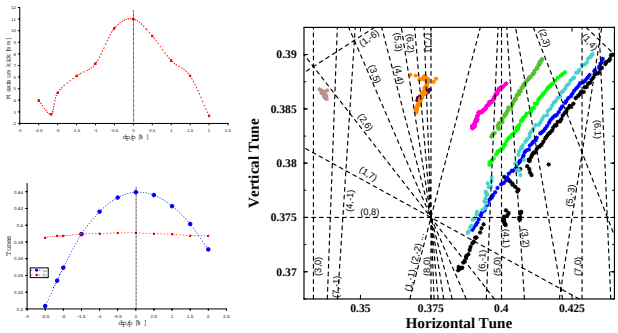

Figure 3: Maximum horizontal kick amplitude in mm (top left), tunes versus momentum spread (bottom) and experimental off-momentum frequency maps (right).

an additional modulation with the sychnotron tune (see [6] and references therein). Ideally, an accurate tune determination in a very small number of turns is needed in order to overturn the problem. This is possible if there is a number of BPMs which are symmetric with respect to the ring optics and thereby their azimuthal position. In the ideal case, where the optics is completely symmetric, the use of data from N symmetric BPMs per turn represents just a "time" rescaling and the new tune Q_N is given by $Q_N = \mathrm{frac}(Q/N)$, i.e. the fractional part of betatron tune divided by the number of BPMs. Preliminary analytical and numerical results have also shown that even in the realistic case of distorted beam optics or non symmetrically spaced BPMs, the accurate tune recovery is still possible. An experimental proof, is shown in Fig. 4, where the average horizontal and vertical tune using data from all symmetric BPMs of the ESRF storage ring (9 families out of 14) is plotted versus the number of turns (each turn includes 16 position measurements). Curves with different colour correspond to different kick amplitudes. The standard deviation shown in the bottom represents a good indication of the tune precision which is better than 10^{-4}, for around 20-30 turns. Simulations have also shown that a data interpolation by using a "virtual BPM" can slightly increase the precision. By using this analysis, a significant gain in

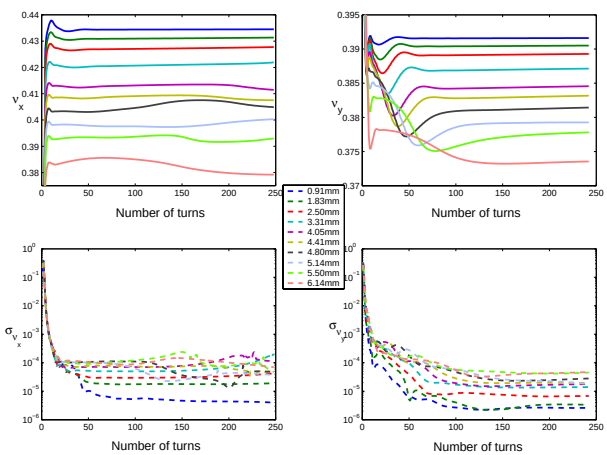

Figure 4: Average horizontal (left) and vertical (right) tune (top) and standard deviation (bottom) measured by using 9 families of 16 symmetric BPMs versus the number of turns.

acquisition time (a factor of 10) can be achieved, for the standard MTOUR system (typically recording 256 turns).

MEASUREMENTS WITH LONGITUDINAL KICKS

Measurements of TBT data with longitudinal beam excitations coupled with transverse kicks were also performed. The longitudinal kicks are produced by pulsing an RF phase shifter in a step like form of 300 μs. The strength of the kicks are very large but presently uncalibrated. When the synchrotron phase is left oscillating, a transverse kick is applied. The beam transverse oscillations are recorded by both BPM systems. An example of the horizontal position recorded in a dispersive BPM is given in Fig. 5, where we observe the transverse oscillations to be modulated by sychnotron oscillations. This is also visible in the Fourier spectrum, where apart from the dominant horizontal tune, the sychnotron tune, as well as sychnotron sidebands coupled with the horizontal tune appear. The dedicated ADAS BPM can also provide a phase signal which is pictured in the right part of Fig. 5.

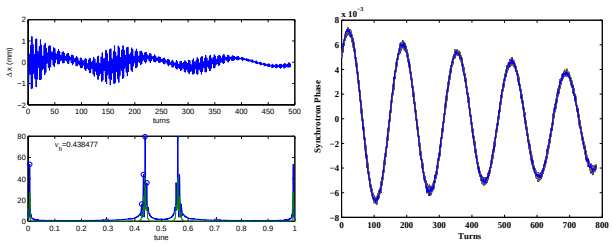

Figure 5: Horizontal amplitude in mm recorded in a dispersive BPM and associated spectrum (left) and phase signal recorded in a stripline (ADAS system).

One straightforward application of the longitudinal kick measurements is the determination of the sychnotron tune, with normalised precision of better than 10^{-3}, which can be used for calibrating the RF voltage read-out. The energy kicks can be calibrated by using the horizontal position and the dispersion measured through a classical RF phase scan. After calibration, the dispersion can also be measured in only one kick (Fig. 6 right). The Fourier amplitude of the transverse tune is associated to the beta function. Its variation around the ring determines the off-momentum beta beating (Fig. 6 left). On the other hand, it can be shown [7] that the Fourier amplitude of nQ_s (n an integer) is associated with dispersion η_n of order n. In particular, the Fourier amplitude of $2Q_s$ is $A_{2s} = \frac{1}{4}\eta_2(s)\sigma_\delta^2 l^2$ where σ_δ^2, the sigma of the energy distribution and l the strength of the longitudinal kick. The average measured Fourier amplitude over symmetric cells around the ESRF ring is shown on the right side of Fig. 7. The error bars correspond to one standard deviation and are associated to second order dispersion beating. Finally, one of the most promising measurements is shown in the left side of Fig. 7. The difference of the sychnotron side-bands' Fourier phases ψ_k with the phase of the main tune ψ_0, is

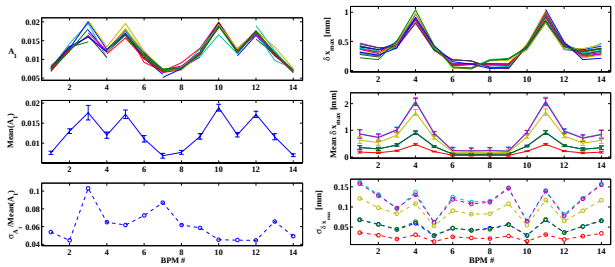

Figure 6: Horizontal tune Fourier amplitude associated to horizontal off-momentum beta function and its variation around the ring (left) and horizontal amplitude variation associated to dispersion beating (right).

$\psi_k - \psi_0 = -|k| \arctan(\frac{lQ_s}{Q'\sigma_\delta})$, i.e. proportional to the order k [7]. The proportionality factor depends on the chromaticity Q'. The longitudinal kicks being uncalibrated, we are not able to give an exact value for the chromaticity. On the other hand, Fig. 7 demonstrates that indeed the dependence of the phase difference is linear with k. Nevertheless, the slope is not symmetric with respect to zero. This may be attributed to the fact that the longitudinal kicks applied were quite large and the formula above should be corrected, taking into account the off-momentum optics beating (as in the case of the side-band Fourier amplitudes [7]).

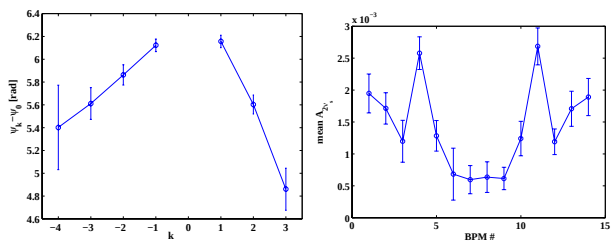

Figure 7: Phase difference of sychno-betatron side-bands versus their order (left) and mean amplitude of the spectral line $2Q_s$ associated to second order dispersion.

We would like to thank V. Serriere, T. Perron and the ESRF operation group for their help in the course of these experiments, and, G.Rumolo and R.Tomás for discussions.

REFERENCES

[1] J. Laskar, Astron. Astroph. 198, 341, 1988; Icarus 88, 266, 1990; Physica D 67, 257 1993; NATO-ASI, S'Agaro, Spain, 1996; J. Laskar, et al., Physica D 56, 253, 1992; Y. Papaphilippou et al., Astron. Astroph. 307, 427 , 1996; Astron. Astroph. 329, 451, 1998.

[2] H.S. Dumas et al., Phys. Rev. Let. 70, 2975, 1993; J. Laskar et al., Part. Accel. 54, 183, 1996; Y. Papaphilippou, PAC'99, New York, 1999; PAC'01, Chicago, 2001; Y. Papaphilippou et al., PRST-AB 2, 104001,1999; PRST-AB 5, 074001, 2002;

[3] D. Robin et al., Phys. Rev. Let. 85, 558, 2000; L. Nadolski, PhD thesis, CEA, 2001; A.L. Robinson, CERN Courier, Vol 41, N.1, 2001.

[4] Y. Papaphilippou et al., PAC'03, 2003.

[5] L. Farvaque et al., DIPAC 2001, Grenoble, 2001.

[6] M. Furman, in Handbook of Accelerator Physics and Engineering, ed. A. Chao and M. Tigner, p.91.

[7] G. Rumolo, R.Tomás, NIMPRA (in press).